

Influence of the pH on the Complexation of an Amphiphilic Antidepressant Drug and Human Serum Albumin

David Leis, Silvia Barbosa, David Attwood,[†] Pablo Taboada, and Víctor Mosquera*

Grupo de Física de Coloides y Polímeros, Departamento de Física de la Materia Condensada, Facultad de Física, Universidad de Santiago de Compostela, Spain

Received: March 20, 2002; In Final Form: May 23, 2002

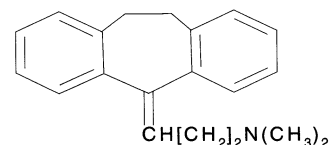
The complexes formed by the interaction of the amphiphilic drug amitriptyline hydrochloride and human serum albumin (HSA) in aqueous solution at pH 3.2, 4.9 (the isoelectric point), and 6.0, were investigated at 25 °C using a range of physicochemical techniques. The complexation process was investigated by conductometric measurements on HSA/amitriptyline solutions of increasing drug concentration from which values of the critical concentration at which adsorption of drug commenced and also the critical micelle concentration of amitriptyline in the presence of protein were determined. The number of adsorption sites was determined from the observed increases of the ζ -potential as a function of drug concentration in the regions of positive ζ -potential where the adsorption was a consequence of the hydrophobic effect. Gibbs energies of adsorption of the drug onto the protein showed an exponential decrease with increase of drug concentration. Measurements of the molar mass and hydrodynamic radius of the HSA–amitriptyline complexes as a function of drug concentration by static and dynamic light-scattering techniques have shown a gradual increase of size typical of a saturation rather than denaturation process. Plots of hydrodynamic radius against amitriptyline concentration have been interpreted by comparison with typical binding isotherms.

1. Introduction

Many drugs, particularly those with local anesthetic, tranquilizing, antidepressant, and antibiotic actions, exert their activity by interaction with biological membranes. In recent papers, we have studied the thermodynamics, aggregation characteristics, and surface properties of several tricyclic antidepressant drugs^{1–4} including that of the present study, amitriptyline hydrochloride. We have shown that the association of this drug in water is characterized by the occurrence of discontinuities in the data from light scattering, ultrasound velocity, specific conductivity, and surface tension at a well-defined critical concentration indicative of a closed association process, and that aggregates of approximately six monomers are formed. The tricyclic antidepressant drugs are a family of structurally similar compounds that possess an almost planar tricyclic ring system with a short hydrocarbon chain carrying a terminal, charged nitrogen atom (see Scheme 1 for structure).

Studies on the structures and interactions of the complexes formed between proteins and surface-active molecules in aqueous solutions by a variety of experimental methods have been extensively reviewed.^{5–8} In general, the amphiphilic molecules chosen for these studies have been ionic surfactants, in view of their application in the area of membrane studies.^{9,10} There is evidence that the initial interaction between ionic surfactants and proteins is predominantly ionic.^{11,12} These initial interactions can cause the protein to unfold, so exposing more binding sites. The existence of nonpolar amino acid side chains on protein molecules suggests the possibility of interaction between proteins and small molecules containing hydrocarbon

SCHEME 1



chains, such as hydrocarbons themselves, simple amphiphiles, or biological lipids.⁵ This hydrophobic interaction between proteins and ionic surfactants can give rise to a conformational change even when the concentration of the ligands is remarkably low.¹³ At surfactant concentrations well below the cmc, micelle-like aggregates start to be adsorbed by the protein or polymer at a critical aggregation concentration (cac), which may be detected from inflection points on the conductivity versus amphiphile concentration plot, similar to those at the cmc of the amphiphile itself. Saturation of the binding sites generally occurs below the critical micelle concentration of the surfactant¹⁴ and results in the appearance of micelles in solution.

The globular protein serum albumin has been widely used as a model protein for studying the interaction between proteins and different surface substrates.¹⁵ Human serum albumin (HSA) consists of 585 amino acids in a single polypeptide chain with a molar mass of 66411 g mol⁻¹ and an isoelectric point¹⁶ of 4.9. Change in pH alters the charge distributions within protein molecules and hence their stability and tendency for surface adsorption.¹⁷ The transition of the globular conformation of serum albumin in bulk solution under different pH conditions has been examined using various techniques including sedimentation, viscosity measurements, small-angle X-ray scattering (SAXS), and small-angle neutron scattering (SANS).^{18–21} HSA is an asymmetric heart-shaped molecule with sides of 8 nm and a thickness of 3 nm that can be roughly approximated as an equilateral triangle with an altitude of 6.9 nm. The two heart

* Author to whom correspondence should be addressed. Tel: 0034981563100, ext. 14056. Fax: 0034981520676. E-mail: fmvector@usc.es.

[†] School of Pharmacy and Pharmaceutical Sciences, University of Manchester, Manchester M13 9PL, U.K.

“lobes” contain HSA’s two binding sites, which consist almost exclusively of hydrophobic side chains, while the outside of the molecule contains most of the polar groups. The tip of the heart is positively charged at physiological pH. Most of the studies have shown that over the pH range between 5 and 7, the proteins are predominantly ellipsoidal with approximate dimensions of $4 \times 4 \times 14 \text{ nm}^3$. The globular structure is composed of three main domains that are loosely joined together through physical forces and six subdomains that are wrapped by disulfide bonds. It is thus expected that upon adsorption some possible structural deformation may occur as a result of either the interaction between protein molecules and the substrate, steric or electrostatic effects within the adsorbed layer, or a combination of both processes. Strong interaction can deform the globular framework, leading to a complete breakdown of the globular integrity.

HSA constitutes approximately half of the total blood protein, acting as a carrier for fatty acids and several amphiphiles from bloodstream to tissues, and hence is an appropriate choice of protein for a study of interaction with amphiphilic drugs. The main aim of this work was to study the nature of the complex formed between amitriptyline and the globular protein HSA at different pH conditions, with a view to elucidating the effect of hydrophobic and electrostatic interaction between the amphiphilic amitriptyline molecule and the protein as a function of pH change. The change in pH will affect the distribution of charges within protein molecules and hence also the electrostatic interaction within an adsorbed layer and the degree of hydration of protein molecules at the interface. As in our previous analysis of the interactions of amphiphilic penicillins and HSA,^{22–24} we have used conductivity measurements to monitor changes in the onset of the self-association of amitriptyline caused by its adsorption on the albumin molecules at pH above, below, and at the isoelectric point of the protein (amitriptyline hydrochloride is fully ionized at the pH of the solutions). The electrophoretic mobility of the serum albumin–amitriptyline complex was measured over a wide range of drug concentration providing information on the adsorbed layer, the ζ -potential of the complex, and the energies of adsorption. We have also used a UV difference spectroscopy technique²⁵ to detect any induced conformational changes in the protein that affect the amino acid residues located on the surface of the proteins. Finally, we characterized the HSA/drug complex using static (SLS) and dynamic (DLS) light-scattering techniques.

2. Experimental Section

2.1. Materials. Human serum albumin (70024-90-7, 98% purity) and amitriptyline (3-(10,11-dihydro-5H-dibenzo[*a,d*]-cyclohepten-5-ylidene)-*N,N*-dimethylpropylamine monohydrochloride) hydrochloride of at least 98.5% purity were purchased from Sigma Chemical Co. and used without further purification. Experiments were carried out using double distilled and deionized water.

2.2. Adsorption of Amitriptyline onto Human Serum Albumin. Aliquots of 2.5 cm^3 of a stock solution of HSA were added to equal volumes of solutions of the drug to give solutions in which the final concentration of albumin was 0.125% w/v and that of the amitriptyline covered the required range. The solutions were maintained at 25°C until equilibrium adsorption onto the protein was achieved.

2.3. Preparation of Buffer Solutions. The buffers used were glycine (0.05 mol dm^{-3})–hydrochloride acid for pH 3.2 (ionic strength $0.0312 \text{ mol kg}^{-1}$); sodium acetate–acetic acid for pH 4.9 (ionic strength $0.080 \text{ mol kg}^{-1}$); and Na_2HPO_4 and NaH_2PO_4 for pH 6.0 (ionic strength $0.085 \text{ mol kg}^{-1}$).

2.4. Conductometric Measurements. Conductivities of solutions of drug and drug/protein complex were measured with a HP 4285A Precision LCR meter equipped with a HP E5050A colloid dielectric probe. The probe is especially designed to measure inductances and to avoid the polarization that occurs when the probe is constructed from plain condenser plates. The amitriptyline solution was progressively added with a 665 Dosimat Meltron peristaltic pump to HSA solution (0.125% w/v) in a water bath to maintain the temperature at $25 \pm 0.01^\circ\text{C}$ and the conductance was measured after thorough mixing and temperature equilibrium.

2.5. ζ -Potential Measurements. ζ -potentials of the HSA/amitriptyline complexes were measured using a Zetamaster 5002 (Malvern Instruments Ltd) by taking the average of five measurements at stationary level. The cell used was of $5 \text{ mm} \times 2 \text{ mm}$ rectangular quartz capillary. The temperature of the experiments was $25.0 \pm 0.1^\circ\text{C}$ controlled by a water bath.

2.6. Static Light-Scattering (SLS). Measurements were made at $25.0 \pm 0.1^\circ\text{C}$ and at a scattering angle of 90° using a BI-200SM Brookhaven laser light-scattering instrument equipped with a 4-W argon ion laser (Coherent Innova 90) operating at 488 nm with vertically polarized light. The intensity scale was calibrated against benzene. Solutions were clarified by ultra-filtration through $0.1 \mu\text{m}$ Millipore filters, until the ratio of light scattering at angles of 45° and 135° did not exceed 1.10. The temperature of the experiments was $25.0 \pm 0.1^\circ\text{C}$ controlled by a water bath.

2.7. Dynamic Light Scattering (DLS). Dynamic light-scattering measurements were made under similar conditions as for SLS by means of the Brookhaven equipment described above in combination with a Brookhaven BI 9000AT digital correlator with a sampling time range of 25 ns to 40 ms. The correlation functions from dynamic light scattering were analyzed by the constrained regularized CONTIN method,²⁶ to obtain distributions of decay rates (Γ). Experiment duration was in the range 5–15 min, and each experiment was repeated at least twice. The decay rates gave distributions of the mutual-diffusion coefficients (D_m) of the HSA/drug complex that were used to evaluate the apparent hydrodynamic radius ($r_{h,\text{app}}$, radius of the hydrodynamically equivalent hard sphere corresponding to D_m) via the Stokes–Einstein equation: $r_{h,\text{app}} = k_B T / 6\pi\eta D_m$, where k_B is the Boltzmann constant and η is the viscosity of the solvent at temperature T . The temperature of the experiments was $25.0 \pm 0.1^\circ\text{C}$ controlled by a water bath.

2.8. Difference UV–Vis Spectroscopy. Difference spectra were measured using a Beckman spectrophotometer (model DU 640), with six microcuvettes, operating in the UV–visible region, with a full-scale expansion of 0.2 absorbance units. For absorbance difference spectra, five of the six microcuvettes were filled with protein/drug solutions; the remaining microcuvette contained only protein in the corresponding medium and was used as a blank reference. All the measurements were made using serum albumin solutions of concentration 0.125% w/v in each of a pair of carefully matched quartz microcuvettes and at pH 3.2, 4.9, and 6.0. The microcuvettes were filled and placed in the same orientation for all tests. Absorbance was measured at 25°C using a temperature controller (Beckman DU series) based on the Peltier effect.

3. Results and Discussion

3.1. Complexation of Amitriptyline and HSA. 3.1.1. Conductivity. The variation of the excess conductivity, κ_e , of solutions of amitriptyline (after subtraction of the contribution of the buffers to the conductivity) with drug molality, m , in the

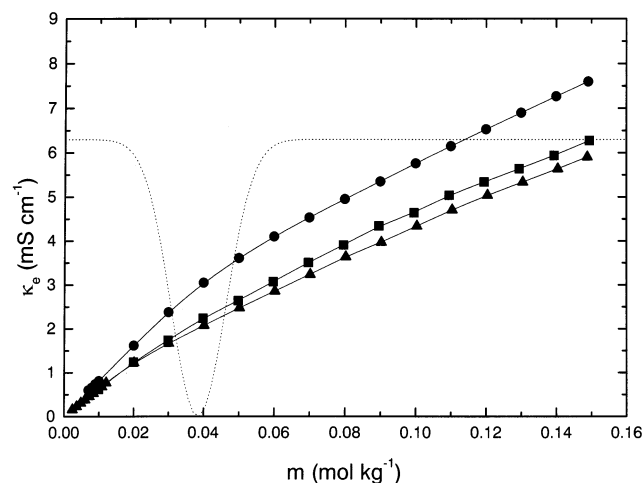


Figure 1. Excess conductivity (in excess of that of buffer solution), κ_e , of amitriptyline as a function of molality at pH (●) 3.2, (■) 4.9, and (▲) 6.0, respectively, at 25 °C. Dashed line represents the second derivative of the conductivity–molality curve at pH 3.2.

TABLE 1: Critical Micelle Concentrations, cmc, of Amitriptyline Hydrochloride in Buffer Solutions, and Critical Aggregation Concentrations, cac, and Critical Micellar Concentration, cmc*, for Amitriptyline Hydrochloride in the Presence of 0.125% w/v of HSA at pH 3.2, 4.9, and 6.0 at 25 °C

pH	cmc (mol kg ⁻¹)	cac (mol kg ⁻¹)	cmc* (mol kg ⁻¹)
3.2	0.039	0.040	0.097
4.9	0.025		0.070
6.0	0.023		0.064

absence of protein at three pH values is shown in Figure 1. The curvature of the plots in the region of the critical micelle concentration (cmc) is a consequence of the low aggregation number of the drug aggregates. Precise values of the cmcs were derived from the plots of conductivity against concentration by an analytical procedure²⁷ based on the Phillips definition of the critical micelle concentration,²⁸ in which the cmc is defined as the concentration corresponding to the maximum change in gradient in plots of the solution conductivity vs concentration: $(d^3\kappa_e/dm^3)_{cmc} = 0$. The procedure involves a Gaussian approximation of the second derivative of the conductivity/concentration data followed by two consecutive numerical integrations by the Runge Kutta method and the Levenberg–Marquardt least-squares fitting algorithm. The figure shows the minimum of the second derivative and, therefore, the cmc of the amitriptyline at pH 3.2; the cmc's at pH 4.9 and 6.0 were determined by a similar procedure (see Table 1). The decrease of cmc between pH 3.2 and 4.9 is a consequence of a higher ionic strength of the buffers used at the higher pH rather than a direct effect of pH on the self-association of amitriptyline, which is fully ionized over this pH range ($pK_a = 9.4$).²⁹

Figure 2 shows plots of the excess conductivities of solutions of amitriptyline in the presence of 0.125% w/v human serum albumin (HSA) as a function of drug concentration at three pHs. The conductivity vs concentration plot at pH 3.2 (below the isoelectric point) shows four linear regions giving rise to three break points. The first break point is interpreted as the critical aggregation concentration (cac), which signals the onset of adsorption of drug and formation of the drug/protein complex. At this pH the protein is positively charged and interactions with the cationic drug are hydrophobic. The second inflection, is the critical micelle concentration (cmc*) of the drug in the presence of drug/protein complex, and corresponds to the point

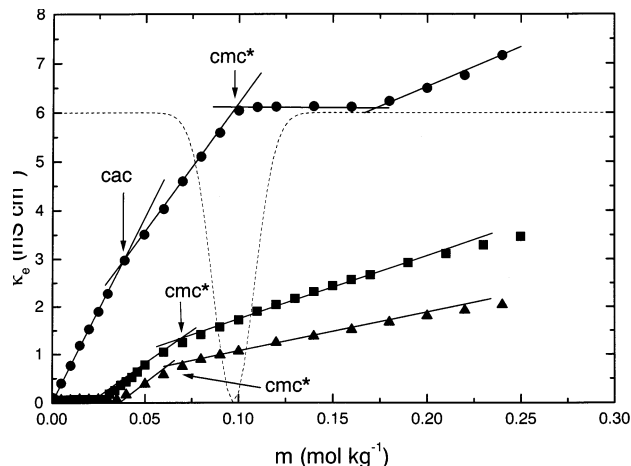


Figure 2. Excess conductivity (in excess of that of buffer solution), κ_e , of HSA (0.125% w/v)/amitriptyline vs molality of amitriptyline at pH (●) 3.2, (■) 4.9, and (▲) 6.0. Dashed line represents the second derivative of the conductivity–molality curve at pH 3.2.

of saturation of the protein surface (as seen also from the ζ -potential and DLS measurements below). The difference in values of cmc* and cmc (Table 1) is, of course, a consequence of the removal of drug molecules from solution by their adsorption by the HSA. The constant conductivity between the second and third inflections might be a consequence of the dense cloud of counterions associated with the hydrophobically bound drug that now surrounds the complex and restricts its mobility.^{30,31} The third break corresponds to an unfolding or conformational change of the protein complex, and is also observed in plots of hydrodynamic radius against drug concentration as discussed in Section 3.1.3. At pH 4.9 and 6.0 the protein and the drug monomers have opposite charge and there is electrostatic interaction between drug and protein resulting in more extensive adsorption of drug; hence the lower conductivities compared to the plot at pH 3.2. The conductivities are close to zero at concentrations lower than 0.025 (pH 4.9) and 0.035 mol kg⁻¹ (pH 6.0) because of almost complete removal of charged drug and counterions from solution by adsorption to form a protein/drug complex with a shell of counterions and consequent limited mobility. Only hydrophobic interactions occur at higher drug concentrations, and the presence of free ions (cations and counterions) in solution causes an increase of conductivity. The critical micelle concentration is detected as an inflection in the κ_e vs m plots at the values given in Table 1.

3.1.2. Electrokinetic Behavior of the HSA/Amitriptyline Complex. Electrostatic interactions play an important role in protein adsorption. In calculating the ζ -potential of a small particle (as here), the deformation of the applied field by the presence of the particle in its neighborhood can be neglected. Moreover, it may also be assumed that the electrophoretic retardation does not affect the particle to any great extent, and the only retarding force on the particle is the viscous drag from the water. As the protein charge is low, and electrophoresis is carried out at normal ionic strengths, the ζ -potential of such particles can be expected to be low. Consequently, although the relaxation effect is relatively unimportant, the electrophoretic retardation should not be neglected.³²

The ζ -potentials of the HSA/amitriptyline complexes were calculated from the electrophoretic mobility, u , assuming protein radii, a , of approximately 3.7, 3.5, and 3.1 nm at pH 3.2, 4.9, and 6.0, respectively, (from light-scattering data below) using the Henry correction of Smoluchowski's equation:³³

$$\zeta = \frac{3\eta u}{2\epsilon_0\epsilon_r f(\kappa a)} \quad (1)$$

where the permittivity of vacuum, ϵ_0 , the relative permittivity of the medium, ϵ_r , and the viscosity of water, η , were taken as $8.854 \times 10^{-4} \text{ J}^{-1} \text{ C}^2 \text{ m}^{-1}$, 78.5, and $8.904 \times 10^{-4} \text{ N m}^{-2} \text{ s}$, respectively. $f(\kappa a)$ is the Henry coefficient that depends on the particle shape; for a sphere with $\kappa a > 1$ it is given by

$$f(\kappa a) = \frac{3}{2} - \frac{9}{2\kappa a} + \frac{75}{2\kappa^2 a^2} - \frac{330}{\kappa^3 a^3} \quad (2)$$

κ being the reciprocal Debye length.

Figure 3 shows the ζ -potential of the HSA/amitriptyline complex at the three pH values as a function of drug concentration. At pH 3.2, the plot shows an initial decrease of the ζ -potential (a reduction of the protein charge) with increase of drug concentration. Sabaté et al.³¹ reported a similar result in solutions *n*-alkyltrimethylammonium bromides and the hydrolytic enzyme α -amylase. The decrease is a consequence of extensive adsorption of counterions and some drug monomers in the double layer around the protein molecules due to the exposure of specific binding sites from the inner core of the molecule as a consequence of a more extended configuration of the HSA structure in an acid medium.^{34–36} At higher drug concentrations the ζ -potential increases with concentration to a constant value representing saturation of the protein surface. Similar increases of ζ -potential with amitriptyline concentration to a plateau value are observed at the two higher pH values, and at pH 6.0 are accompanied by a change in the sign of the ζ -potential as the cationic drug molecules are progressively adsorbed onto the protein during the initial phase.

The surface charge density enclosed by the shear plane, σ_ζ , was obtained from the corresponding ζ -potentials using the following equation for a $z:z$ electrolyte:³⁷

$$\sigma_\zeta = \frac{\epsilon_r \epsilon_0 k_B T \kappa}{ze} \left[2 \sinh \left(\frac{ez\zeta}{2k_B T} \right) + \frac{4}{\kappa a} \tanh \left(\frac{ez\zeta}{4k_B T} \right) \right] \quad (3)$$

where e is the elemental charge, z is the valence of the ion, and k_B is the Boltzmann constant. Equation 3 takes into account the particle curvature and gives surface charge density to within 5% for $\kappa a > 0.5$ for any ζ -potential. The values of the calculated charge are plotted in Figure 4.

Equation 4 can be used to calculate the number of adsorption sites N_1 when the increase of the ζ -potential is due mainly to the hydrophobic interactions,^{38,39} i.e., at pH 3.2,

$$\left(\frac{d\zeta}{d \log m} \right) = \frac{4.606 k_B T}{ze} \left(\frac{\sinh(ze\zeta_1/2k_B T) - \sinh(ze\zeta_2/2k_B T)}{\cosh(ze\zeta_2/2k_B T)} \right) \quad (4)$$

$$\left(\frac{\sqrt{8n_0\epsilon_r\epsilon_0 k_B T} [\sinh(ze\zeta_1/2k_B T) - \sinh(ze\zeta_2/2k_B T)]}{zeN_1} - 1 \right)$$

where ζ_1 and ζ_2 are selected ζ -potentials on the graph, and n_0 is the ionic concentration. The number of available adsorption sites per unit area obtained from eq 4 at pH 3.2 was $8.8 \times 10^{14} \text{ m}^{-2}$.

The adsorption constant k_2 was calculated from

$$\frac{1}{m} = k_2 \left(\frac{zeN_1}{\sqrt{8n_0\epsilon_r\epsilon_0 k_B T} [\sinh(ze\zeta_1/2k_B T) - \sinh(ze\zeta_2/2k_B T)]} - 1 \right) \quad (5)$$

Here m is chosen as the concentration at the ζ -potential midpoint between ζ_1 and ζ_2 .

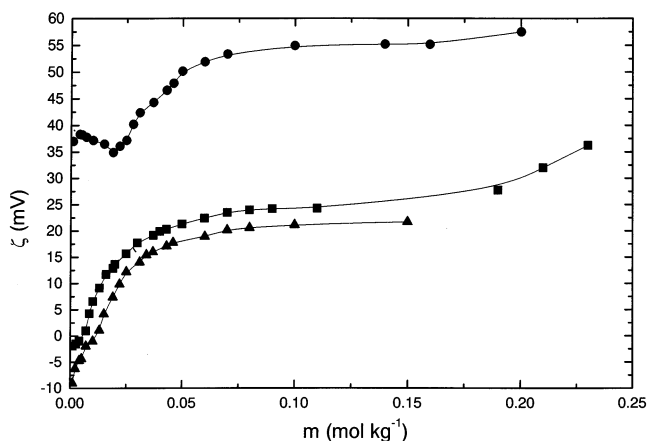


Figure 3. ζ -potential of HSA (0.125% w/v) as a function of amitriptyline molality at 25 °C at pH (●) 3.2, (■) 4.9, and (▲) 6.0.

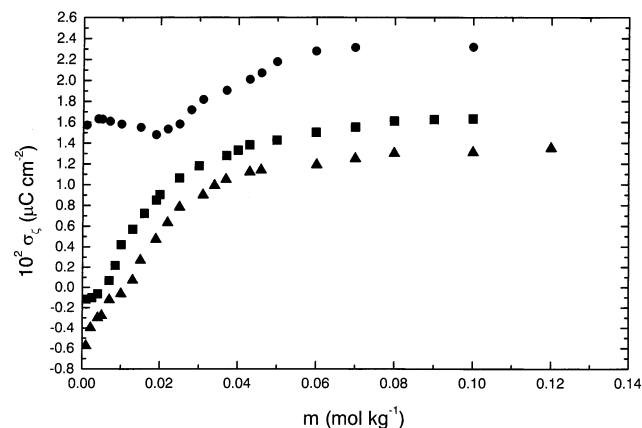


Figure 4. Surface charge density enclosed by the shear plane, σ_ζ , as a function of amitriptyline molality at 25 °C and pH (●) 3.2, (■) 4.9, and (▲) 6.0.

At pH 4.9 and 6.0, electrostatic interactions during the adsorption process must be considered and for that reason the number of adsorption sites and the adsorption constant were calculated from the Ottewill–Watanabe model,⁴⁰ which takes into account the electrostatic interactions and is based on the Langmuir adsorption isotherm. In this model it is assumed that the surfactant adsorption does not affect the potential-determining ions and the differences between the charge densities on the ion, $\Delta\sigma_i$, and on the diffuse layer, $\Delta\sigma_d$, before and after adsorption of the drug can be expressed as

$$-\Delta\sigma_d = \sigma_i = \frac{k_1 m}{1 + k_2 m} \quad (6)$$

where $k_1 = zeN_1 k_2$. From the ζ – $\log m$ plots at the point of zero charge (pzc) we have

$$\left(\frac{d\zeta}{d \log m} \right)_\zeta = 0 = 2.303 \zeta^0 \left[\frac{\epsilon_0 D (1 + \kappa a) \zeta^0}{a N_1 z e} - 1 \right] \quad (7)$$

$$\frac{1}{m_0} = k_2 \left[\frac{a z e N_1}{\epsilon_0 D \zeta^0 (1 + \kappa a)} - 1 \right] \quad (8)$$

where m_0 is the surfactant molality at the pzc, ζ^0 is the ζ -potential in the absence of drug, and $D = 4\pi\epsilon_r\epsilon_0$. Equations 7 and 8 can be simultaneously solved to obtain values of N_1 and k_2 . The values of N_1 obtained in this way were 1.95×10^{16} and $1.03 \times 10^{17} \text{ m}^{-2}$ at pH 4.9 and 6.0, respectively, which are

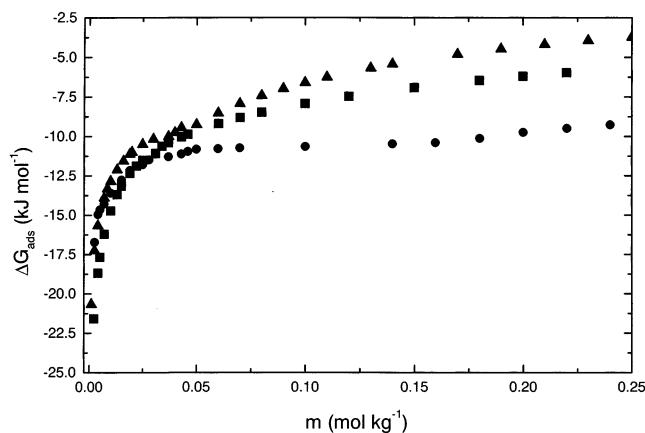


Figure 5. Gibbs energy of adsorption, ΔG_{ads}^0 , of the HSA (0.125% w/v)/amitriptyline calculated by the Kayes approximation as a function of amitriptyline molality at 25 °C and pH (●) 3.2, (■) 4.9, and (▲) 6.0.

of magnitude similar to those obtained for other amphiphilic cationic drug–protein complexes. For example, values of N_1 for the propranolol hydrochloride/HSA system from ζ -potential studies⁴¹ were 1.3×10^{16} and $1.5 \times 10^{17} \text{ m}^{-2}$ at pH 4.9 and 8.0, respectively, and $5.48 \times 10^{15} \text{ m}^{-2}$ from capillary electrophoresis/frontal analysis measurements.⁴²

The standard free energy of adsorption, ΔG_{ads}^0 , may be obtained from k_2 using the relationship

$$k_2 = \exp(-G_{\text{ads}}^0/k_B T) \quad (9)$$

Representative plots of the standard Gibbs energies of adsorption evaluated from the k_2 values of eqs 5 and 8 are shown in Figure 5. At pH 3.2 calculations were restricted to hydrophobic interactions. ΔG_{ads}^0 values evaluated in this manner are large and negative at low antidepressant concentrations where binding to the high-energy sites takes place and become less negative as more drug molecules bind, suggesting a saturation process. Similar behavior was reported for the systems penicillin–HSA,^{22–24} propranolol–HSA,⁴¹ propranolol–haemoglobin,⁴¹ and verapamil–HSA.⁴³ An additional increment of ΔG_{ads}^0 at concentrations above the cmc^* suggests unfolding of the complex, in agreement with the ζ -potential results and the DLS data discussed in Section 3.1.3.

3.1.3. Light Scattering. (A) Data Analysis. In dynamic light scattering the intensity–intensity autocorrelation function is measured and related to the normalized electric field autocorrelation function, $g_1(t)$ by the Siegert relation:

$$g_2(t) - 1 = \beta |g_1(t)|^2 \quad (10)$$

where β is a factor that accounts for derivations from ideality.

The parameter $g_1(t)$ can be written as the Laplace transform of the distribution of relaxation rates, $G(\Gamma)$:

$$g_1(t) = \int_0^\infty G(\Gamma) \exp(-\Gamma t) d\Gamma \quad (11)$$

where Γ is the relaxation rate. For relaxation times, τ , the parameter $g_1(t)$ is expressed as

$$g_1(t) = \int_0^\infty \tau A(\tau) \exp(-t/\tau) d \ln \tau \quad (12)$$

where $\tau A(\tau) \propto \Gamma G(\Gamma)$. To obtain $\tau A(\tau)$, the DLS data were analyzing using the inverse Laplace transform routine CONTIN and presented as plots of intensity against decay time.

The static light-scattering data were analyzed using the classical Debye equation:

$$\frac{Kc}{R(\theta)} = \frac{1}{M_w} + 2A_2c(c \rightarrow 0, \theta \rightarrow 0) \quad (13)$$

where $R(\theta \rightarrow 0)$ is the Raleigh ratio at an angle θ tending to zero (due to the small size of the particles, the condition is achieved at $\theta = 90^\circ$), c is the drug concentration (g cm^{-3}), M_w is the molar mass, A_2 is the second virial coefficient, and K is an optical constant depending on the apparatus and on the particles analyzed:

$$K = \frac{4\pi n_s^2}{N_A \lambda_0^4} \left(\frac{\partial n}{\partial c} \right) \quad (14)$$

where n_s is the refractive index of the solution, $\partial n/\partial c$ is the refractive index increment of the solution ($0.0738 \text{ kg mol}^{-1}$), N_A is the Avogadro's number, and λ_0 is the wavelength of the incident light in a vacuum. The dissymmetry ratio (scattering intensity at 45° relative to that at 135°) was near unity and measurements were carried out at $\theta = 90^\circ$. In the analysis of SLS data, it was assumed that the increase in scattering was attributable to an increase in complex size due entirely to the adsorption of drug, any aggregation of the complexes was assumed to be negligible, and the concentration region avoided the cmc^* . This assumption seems reasonable since the sample polydispersity indexes (the variance divided by the square of the average) from dynamic light-scattering measurements for this system were low in the concentration used for the static light-scattering measurements, indicative of a reasonable degree of monodispersity of size of the scattering units.

It is known that charged proteins present additional problems associated with interpretation of light-scattering data from aqueous systems composed of electrolyte and a diffusible species interacting with it. Such problems arise from (i) the contribution of charged fluctuations to the intensity of the scattered light, and (ii) the preferential interaction to the $\partial n/\partial c$ term of eq 14. The first problem is usually avoided by operating at constant ionic strength, and the second problem may be solved by operating at a constant chemical potential, μ , of all diffusible species, including in this case the drug. In practice, this was achieved by carrying out dialysis equilibrium prior to the scattering experiment and $(\partial n/\partial c)_\mu$ measurements.^{44,45}

The molar mass obtained using the Debye equation for the HSA in pure water was $7.75 \pm 0.1 \times 10^4 \text{ g mol}^{-1}$, which corresponds to an association number $N' = M_w/M_0$ (where M_0 is the molecular weight of the HSA, $6.641 \times 10^4 \text{ g mol}^{-1}$) of 1.17 indicating only limited association.

Virial coefficients reflect deviations from ideality due to the existence of intermolecular interactions, the second virial coefficient, A_2 , being related to the pair interactions between molecules. The second virial coefficients obtained from the fit of the experimental data are positive, as shown in Table 2, indicating that the effective interaction between complexes is repulsive and hence there is not a tendency to form association products. Decreases in values of A_2 and increases in values of the number of cationic drug molecules adsorbed, N_0 , with increasing pH is in accordance with the isoelectric point of HSA, 4.9, and the positive charge of the amitriptyline molecule.

(B) Dynamic Light Scattering (DLS). Figure 6 shows selected intensity–decay times of the amitriptyline/HSA complex at pH 6.0 below and above the cmc^* . The distributions obtained for solutions at concentrations below cmc^* showed a single peak

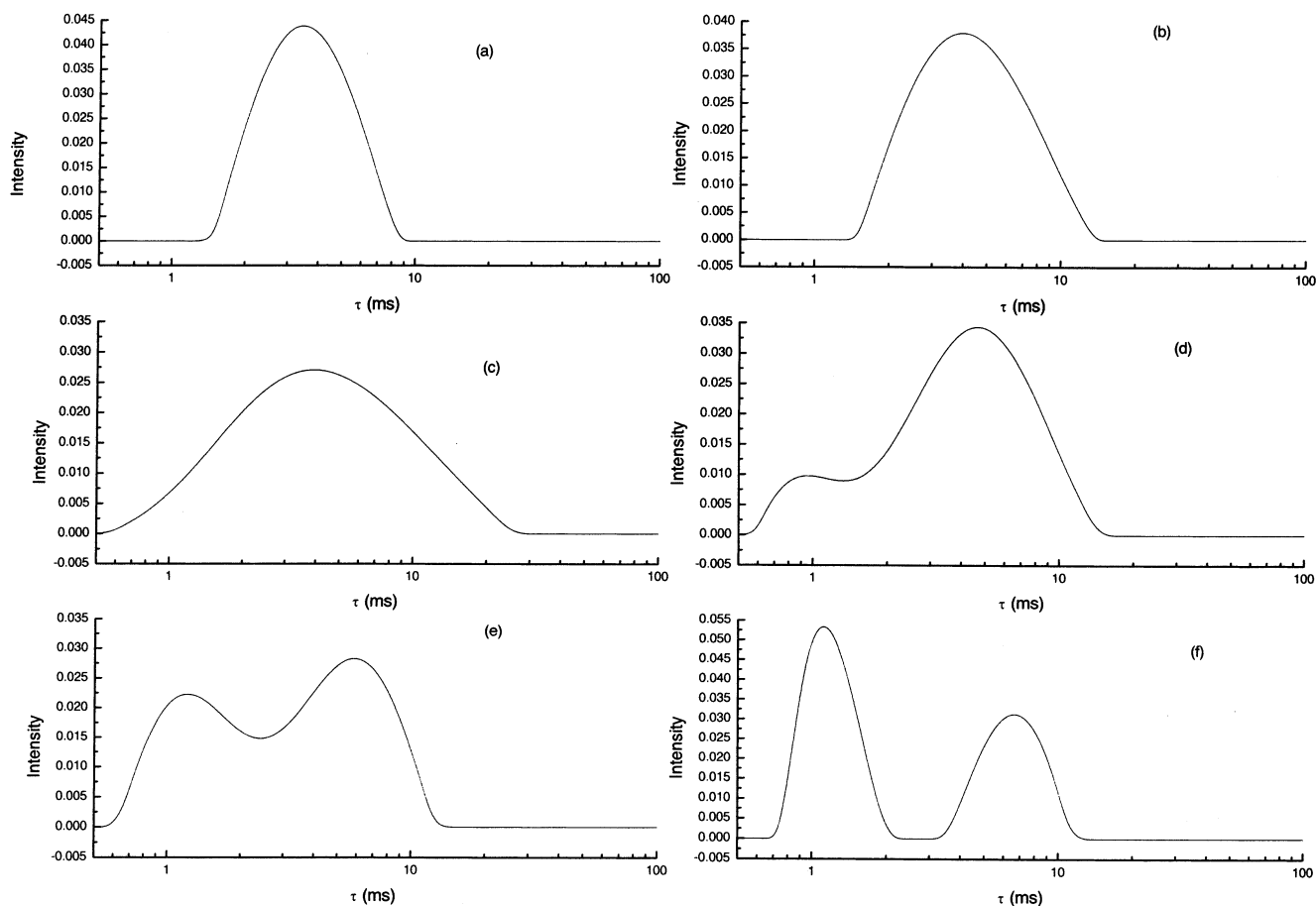


Figure 6. Decay time distribution, τ , in aqueous solutions of HSA (0.125% w/v) and amitriptyline concentrations of (a) 0, (b) 0.016, (c) 0.06, (d) 0.1, (e) 0.14, (f) 0.22 mol kg⁻¹ at pH 6.0.

TABLE 2: Molecular Masses, M_w , Second Virial Coefficients, A_2 , for Amitriptyline–HSA System (0.125% w/v of HSA) and the Number of Molecules of Amitriptyline Adsorbed, N_0 , on the HSA Molecule at 25 °C and pH 3.2, 4.9, and 6.0

pH	$10^3 M_w$ (g mol ⁻¹)	$10^{-3} A_2$ (mol cm ³ g ⁻²)	N_0
3.2	5.9	18	18
4.9	8.7	7	28
6.0	19.3	2	62

corresponding to the complex, which broadened as the concentration of drug increased (Figure 6a–c). The intensity fraction profile at higher concentrations, (Figure 6d,e), showed two overlapping peaks arising from the coexistence of a small number of drug aggregates of low aggregation number, and the complexes. The CONTIN method was unable to provide an exact “two-peak” solution corresponding to these two different species in solution and the approximate hydrodynamic radius of the complex was derived by fitting to a two-exponential function to these data. Two separate peaks could be distinguished by the CONTIN model at concentrations well above the cmc^* , (Figure 6f), with apparent hydrodynamic radii, $r_{h,\text{ap}} \approx 4.5\text{--}5.7$ nm for the complex and $r_{h,\text{ap}} = 1.2$ nm for the drug aggregates. Similar behavior was also reported for the systems SDS/lysozyme,^{36,46} SDS/bovine serum albumin,⁴⁷ and penicillins/HSA.^{23,24} The intensity of the micelle peak increased relative to that of the complex with increase of drug concentration above cmc^* . The protein is therefore behaving in a manner similar to an adsorption interface, which is energetically more favorable

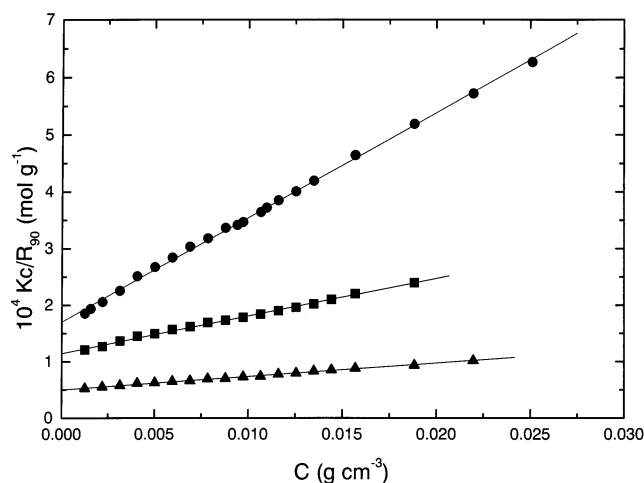


Figure 7. Apparent hydrodynamic radius, $r_{h,\text{ap}}$ of the amitriptyline–HSA complex vs amitriptyline molality for pH (●) 3.2, (■) 4.9, and (▲) 6.0.

than the formation of aggregates, in agreement with the observed higher value of the apparent critical micelle concentrations of the antidepressants in the presence of the protein.

Figure 7 shows an increase of apparent hydrodynamic radii, $r_{h,\text{app}}$, of the amitriptyline–HSA complexes, as a function of the total drug concentration (including both bound and unbound drug) at each pH, as calculated from apparent diffusion coefficients, D_{app} , using the Stokes–Einstein equation. It is interesting to note that the radius of HSA in drug-free solutions at pH 3.2, (3.7 nm), is higher than at pH values 4.9 (3.5 nm) and 6.0 (3.1 nm) in agreement with a previous report.³⁶

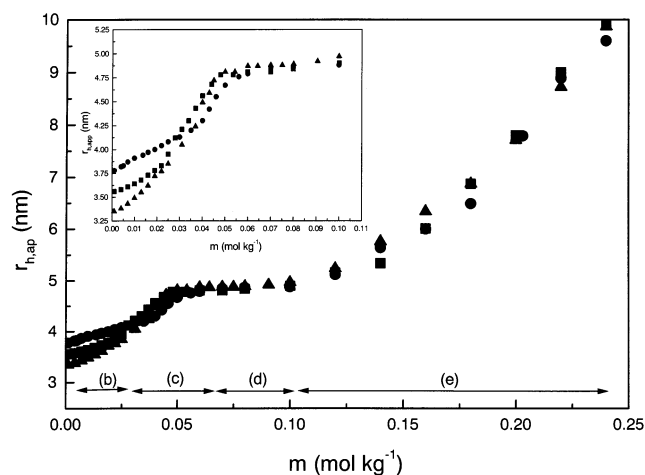


Figure 8. Kc/R_{90} as a function of amitriptyline concentration, c , for the system HSA (0.125% w/v)–amitriptyline in aqueous buffered solutions of pH (●) 3.2, (■) 4.9, and (▲) 6.0.

Figure 7 can be compared to a binding isotherm, showing the average number of surfactant molecules bound per protein molecule as a function of the free surfactant concentration. In general⁴⁸ these display four characteristic regions with increasing surfactant concentration, which may be related to similar changes in Figure 7. Specific electrostatic binding occurs at very low drug concentration (region a, not shown in Figure 7); non cooperative binding (region b) occurs at $m < \sim 0.03 \text{ mol kg}^{-1}$ at each pH; cooperative binding (region c) occurs at concentrations between ~ 0.03 and $\sim 0.06 \text{ mol kg}^{-1}$ in which, as seen from light-scattering data, the hydrodynamic radii increase between 3.5 to $\sim 4.8 \text{ nm}$ at each pH and hydrophobic interactions are predominant, as shown by ζ -potential measurements. Saturation of the surface (region d) occurs at concentrations ranging between ~ 0.06 and $\sim 0.10 \text{ mol kg}^{-1}$, where the hydrodynamic radii remain constant at a value of $\sim 4.8 \text{ nm}$ at each pH. There is an extra zone, (region e), that commences above the cmc* ($m \sim 0.10 \text{ mol kg}^{-1}$), in which the protein starts to unfold. In this zone the increase of the hydrodynamic radii might be a consequence of a more opened expanded structure of the human albumin molecules caused by the binding of a greater amount of drug, as in the case of lysozyme–SDS system,³⁷ producing at least a partial denaturation or a change in the configurational structure of the protein molecules, as indicated by the increase of ζ -potential in this concentration range and by UV–Vis spectra, as will be discussed below.

(C) *Static Light Scattering (SLS).* Figure 8 shows the SLS results for amitriptyline at different pH values at concentrations below the cmc* obtained by conductivity. The solution is considered as a binary system where the HSA buffer solution is regarded as the solvent. Equation 13 provides information on the molar mass, M_w , of the drug bound to the protein (calculated from the difference between the molar mass of the drug/protein complex and that of the HSA itself) and the second virial coefficient, A_2 . The values are shown in Table 2. This table also shows an increase in the average number of amitriptyline molecules adsorbed onto the human serum albumin molecules, N_0 , with increase of pH which is due to increased electrostatic interactions resulting from the difference in net charge between drug and the protein molecules at the higher pH. Virial coefficients reflect deviations from ideality due to the existence of intermolecular interactions. The second virial coefficients, A_2 , are positive, indicating that the effective interaction between complexes is repulsive and hence there is no appreciable tendency for the complexes to associate.

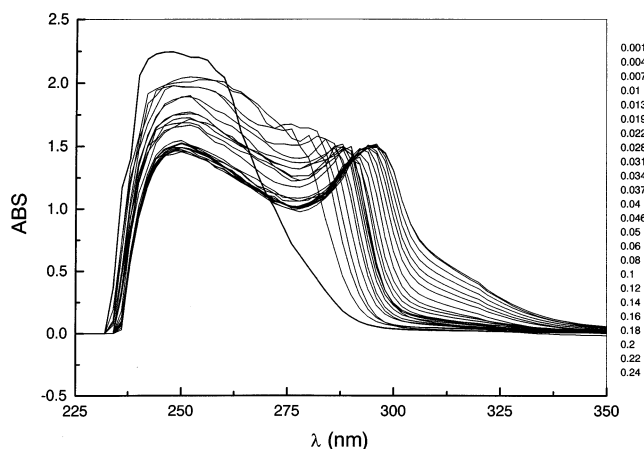


Figure 9. Difference spectra of HSA (0.125% w/v) in the presence of amitriptyline hydrochloride at pH 4.9. The amitriptyline molalities are shown on the plot.

Decreases in the values of A_2 with increasing pH (see Table 2) are mainly a consequence of the decreasing charge of the drug–protein complex due to the more extensive adsorption of drug at higher pH, but there might also be a contribution from changes in the conformations of HSA in the complex with pH change as indicated by the DLS results.

3.1.4. UV–Vis Spectroscopy. Figure 9 shows the difference spectra in the wavelength range 225–350 nm at pH 4.9 between a HSA solution of concentration 0.125% w/v and a solution of HSA of the same concentration containing amitriptyline hydrochloride, at a range of concentrations between 0.003 and 0.24 mol kg^{-1} . Similar plots were obtained for pH values 3.2 and 6.0. The figure shows a broad absorption band with a peak in the region of $\sim 250 \text{ nm}$ corresponding to free amitriptyline molecules, and an additional peak at 288–290 nm at concentrations above the cmc, arising from adsorption of drug onto the protein surface. Drug bound to the protein molecules in the form of micelles, (the necklace model), would induce a change in the molecular structure or a partial denaturation of the protein molecules changing the environment of the protein chromophores (mainly tryptophan and tyrosine) and producing this absorption peak.⁴⁹

It can be observed that as the amitriptyline concentration increases the monomer absorption band decreases as a consequence of the adsorption process and becomes almost constant at concentrations higher than 0.06 mol kg^{-1} . The same trend was obtained at pH 3.2 and 6.0. The peak arising from drug adsorption is detectable at concentrations above 0.03 mol kg^{-1} in accordance with DLS data. Displacement of this peak from 290 to 295 nm with increase of drug concentration corresponds to the formation of free micelles in solution, as indicated by the results obtained by conductivity and DLS. The minimum appearing at 278 nm and a concentration 0.1 mol kg^{-1} may correspond to the unfolding of the protein molecule as indicated from the DLS data. The shoulder on the adsorption peak in the range 310–314 nm, which becomes more pronounced at concentrations above approximately 0.14 mol kg^{-1} , may arise from the formation of transfer complexes.⁴⁹

3.2. Summary

The results presented in this study have characterized the nature of the interaction between the globular anionic protein human serum albumin (HSA) and the cationic drug amitriptyline and have relevance for the transport of this surface active drug in the blood stream. Changes in the ζ -potential and conductivity of amitriptyline/HSA solutions as a function of drug concentra-

tion and of pH have been interpreted in terms of hydrophobic adsorption of this cationic amphiphilic drug on to the surface of HSA at a pH below the isoelectric point. Adsorption commenced at a critical aggregation concentration of 0.040 mol kg⁻¹, saturation of the protein surface occurred at drug concentrations of approximately 0.097 mol kg⁻¹ with further increase of amitriptyline concentration leading to the formation of drug aggregates in solution. There was evidence of an unfolding or conformational change of the drug/protein complex at higher drug concentrations. At pH 4.9 and 6.0 extensive adsorption onto the protein surface occurred at low drug concentration, resulting in a change of sign of the ζ -potential at pH 6.0. Saturation of the surface was noted at concentrations of 0.70 and 0.064 mol kg⁻¹ at pH 4.9 and 6.0, respectively. At each of the three pH values, light-scattering measurements have shown a gradual change in molar mass and hydrodynamic radius of the complex with increasing drug concentration indicative of a saturation rather than a denaturation process.

Acknowledgment. The project was supported by the Ministerio de Ciencia y Tecnología through project MAT2001-2877. P.T. thanks the Ministerio de Educacion y Cultura for his postdoctoral grant.

References and Notes

- (1) Taboada, P.; Attwood, D.; Ruso, J. M.; García, M.; Mosquera, V. *Phys. Chem. Chem. Phys.* **2000**, *2*, 5175.
- (2) Taboada, P.; Attwood, D.; Ruso, J. M.; García, M.; Mosquera, V. *Langmuir* **2001**, *17*, 173.
- (3) Taboada, P.; Ruso, J. M.; García, M.; Mosquera, V. *Colloid Polym. Sci.* **2001**, *279*, 716.
- (4) Taboada, P.; Ruso, J. M.; García, M.; Mosquera, V. *Colloid Surf. A* **2001**, *179*, 125.
- (5) Tanford, C. *The Hydrophobic Effect: Formation of Micelles and Biological Membranes*; Wiley-Interscience: New York, 1980.
- (6) Ananthapadmanabhan, K. P. *Interactions of Surfactants with Polymers and Proteins*; Goddard, E. D., Ananthapadmanabhan, K. P., Eds.; CRC Press Inc.: London, 1993.
- (7) Kwak, J. C. T. *Polymer-Surfactant Systems*; Surfactant Science Series, Vol. 77; Kwak, J. C. T., Ed.; Marcel Dekker: New York, 1998.
- (8) Jones, M. N. In *Biological Thermodynamics*; Jones, M. N., Ed.; Elsevier: Amsterdam, 1988.
- (9) Helenius, A.; Simons, K. *Biochim. Biophys. Acta* **1975**, *415*, 29.
- (10) Jones, O. T.; Earnest, J. P.; McNamee, M. E. Solubilization and Reconstitution of Membrane Proteins. In *Biological Membranes*; Findlay, J. B. C., Evans, W. H., Eds.; IRL Press: Oxford, 1987.
- (11) Oakes, J. J. *Chem. Soc. Faraday Trans. 1* **1974**, *70*, 2200.
- (12) Tipping, E.; Jones, M. N.; Skinner, H. A. *J. Chem. Soc. Faraday Trans. 1* **1974**, *70*, 1306.
- (13) Steinhardt, J.; Reynolds, J. A. *Multiple Equilibria in Proteins*; Academic Press: New York, 1969.
- (14) Jones, M. N. *Biological Interfaces*; Elsevier: Amsterdam, 1975.
- (15) Peters, T. J. *All about Albumin Biochemistry, Genetics, and Medical Applications*; Academic Press: San Diego, CA, 1996.
- (16) Houska, M.; Brynda, E. *J. Colloid Interface Sci.* **1997**, *188*, 243.
- (17) Lu, J. R.; Su, T. J.; Penfold, J. *Langmuir* **1999**, *15*, 6975.
- (18) Bendedouch, D.; Chen, S. H. *J. Phys. Chem. B* **1983**, *87*, 1473.
- (19) Anderegg, J. W.; Beeman, W. W.; Shulman, S.; Kaesberg, P. *J. Am. Chem. Soc.* **1955**, *77*, 2927.
- (20) Squire, P. G.; Moster, P.; O'Konski, C. T. *Biochemistry* **1968**, *7*, 4261.
- (21) Olivieri, J. R.; Craievich, A. F. *Euro. Biophys. J.* **1995**, *24*, 77.
- (22) Taboada, P.; Mosquera, V.; Ruso, J. M.; Sarmiento, F.; Jones, M. N. *Langmuir* **2000**, *16*, 6795.
- (23) Ruso, J. M.; Attwood, D.; García, M.; Taboada, P.; Varela, L. M.; Mosquera, V. *Langmuir* **2001**, *17*, 5189.
- (24) Ruso, J. M.; Taboada, P.; Varela, L. M.; Attwood, D.; Mosquera, V. *Biophys. Chem.* **2001**, *92*, 141.
- (25) Jones, M. N.; Skinner, H. A.; Tipping, E.; Wilkinson, A. E. *Biochem. J.* **1972**, *135*, 231.
- (26) Provencher, S. W. *Makromol. Chem.* **1979**, *180*, 201.
- (27) Pérez-Rodríguez, M.; Prieto, G.; Rega, C.; Varela, L. M.; Sarmiento, F.; Mosquera, V. *Langmuir* **1998**, *14*, 4422.
- (28) Phillips, J. N. *Trans. Faraday Soc.* **1955**, *51*, 561.
- (29) Moffat, A. C. *Clark's Isolation and Identification of Drugs*, 2nd ed.; The Pharmaceutical Press: London, 1986.
- (30) Vasilescu, M.; Angelescu, D.; Almgren, M.; Valstar, A. *Langmuir* **1999**, *15*, 2635.
- (31) Sabaté, R.; Estelrich, J. *Int. J. Biol. Macromol.* **2001**, *28*, 151.
- (32) Bier, M. *Electrophoresis. Theory, Methods and Applications*; Academic Press: New York, 1967.
- (33) Hunter, R. J. *Zeta Potential in Colloid Science*; Academic Press: London, 1981.
- (34) Song, D.; Forcitini, D. *J. Colloid Interface Sci.* **2000**, *221*, 25.
- (35) Luik, A. I.; Naboka, Y. N.; Mogilevich, S. E.; Huscha, T. O.; Mischenko, N. I. *Spectrochim. Acta, Part A* **1998**, *54*, 1503.
- (36) Valstar, A.; Brown, W.; Almgren, M. *Langmuir* **1999**, *15*, 2366.
- (37) Quesada-Perez, M.; Callejas-Fernandez, J.; Hidalgo-Alvarez, R. *Colloids Surf.* **1999**, *159*, 239.
- (38) Kayes, J. B. *J. Colloid Interface Sci.* **1976**, *56*, 426.
- (39) Stadilis, G.; Avranas, A.; Jannakoudakis, D. *J. Colloid Interface Sci.* **1990**, *135*, 313.
- (40) Ottewill, R. H.; Watanabe, A. *Kolloid-Z.* **1960**, *170*, 132.
- (41) Ruso, J. M.; Attwood, D.; García, M.; Prieto, G.; Sarmiento, F.; Taboada, P.; Varela, L. M.; Mosquera, V. *Langmuir* **2000**, *16*, 10449.
- (42) Ding, Y. S.; Zhu, X. F.; Lin, B. C. *Chromatographia* **1999**, *49*, 343.
- (43) Pérez-Rodríguez, M.; Attwood, D.; Ruso, J. M.; Taboada, P.; Varela, L. M.; Mosquera, V. *Phys. Chem. Chem. Phys.* **2001**, *3*, 1655.
- (44) Cassasa, E. F.; Eisenberg, H. *J. Phys. Chem.* **1960**, *64*, 753.
- (45) Cassasa, E. F.; Eisenberg, H. *J. Phys. Chem.* **1961**, *64*, 753.
- (46) Gimel, J. C.; Brown, W. *J. Chem. Phys.* **1996**, *104*, 8112.
- (47) Valstar, A.; Almgren, M.; Brown, W.; Vasilescu, M. *Langmuir* **2000**, *16*, 922.
- (48) Jones, M. N. *Biochem. J.* **1975**, *151*, 109.
- (49) Demchenko, A. P. *Ultraviolet Spectroscopy of Proteins*; Springer-Verlag: Berlin, 1981; Vol. 65, p 427.